

34

## (12) INTERNATIONAL APPLICATION PUBLISHED UNDER THE PATENT COOPERATION TREATY (PCT)

(19) World Intellectual Property Organization  
International Bureau(43) International Publication Date  
18 July 2002 (18.07.2002)

PCT

(10) International Publication Number  
**WO 02/055993 A2**(51) International Patent Classification<sup>7</sup>:**G01N**

(72) Inventor; and

(21) International Application Number:

PCT/US02/00922

(75) Inventor/Applicant (for US only): **GEORGIADIS, Rosina, M.** [US/US]; 250 Tappan Street, Brookline, MA 02445 (US).

(22) International Filing Date: 11 January 2002 (11.01.2002)

(25) Filing Language:

English

(74) Agents: **GAGNEBIN, Charles, L., III et al.**; Weingarten, Schurigin, Gagnebin & Lebovici, LLP, Ten Post Office Square, Boston, MA 02109 (US).

(26) Publication Language:

English

(81) Designated States (national): AE, AG, AL, AM, AT, AU, AZ, BA, BB, BG, BR, BY, BZ, CA, CH, CN, CO, CR, CU, CZ, DE, DK, DM, DZ, EC, EE, ES, FI, GB, GD, GE, GH, GM, HR, HU, ID, IL, IN, IS, JP, KE, KG, KP, KR, KZ, LC, LK, LR, LS, LT, LU, LV, MA, MD, MG, MK, MN, MW, MX, MZ, NO, NZ, OM, PH, PL, PT, RO, RU, SD, SE, SG, SI, SK, SL, TJ, TM, TN, TR, TT, TZ, UA, UG, US, UZ, VN, YU, ZA, ZM, ZW.

(30) Priority Data:

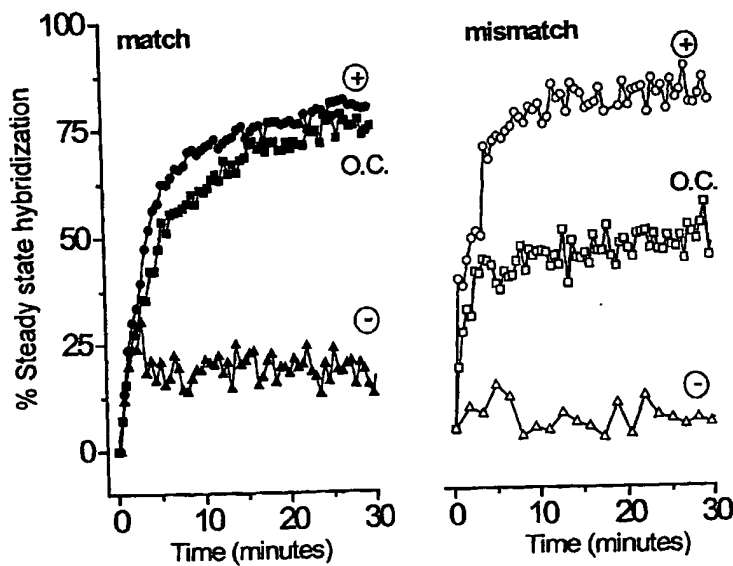
60/261,504 12 January 2001 (12.01.2001) US  
60/340,145 14 December 2001 (14.12.2001) US(71) Applicant (for all designated States except US):  
**TRUSTEES OF BOSTON UNIVERSITY** [US/US]; 147 Bay State Road, Boston, MA 02215 (US).

(84) Designated States (regional): ARIPO patent (GH, GM, KE, LS, MW, MZ, SD, SL, SZ, TZ, UG, ZM, ZW),

(72) Inventor: HEATON, Richard, J. (deceased).

[Continued on next page]

(54) Title: USE OF ELECTROSTATIC FIELDS TO ENHANCE SURFACE PLASMON RESONANCE SPECTROSCOPY

**WO 02/055993 A2**

(57) Abstract: *In-situ* optical surface plasmon resonance spectroscopy (SPR) can be used to monitor hybridization kinetics for unlabeled DNA in tethered monolayer nucleic acid films on gold in the presence of an applied electrostatic field. The DC field can enhance or retard hybridization and can also denature surface-immobilized DNA duplexes. Discrimination between matched and mismatched hybrids is achieved by simple adjustment of the electrode potential. Although the electric field at the interface is extremely large, the tethered ssDNA thiol probes remain bound and can be reused for subsequent hybridization reactions without loss of efficiency. Only capacitive charging currents are drawn; redox reactions are avoided by maintaining the gold electrode

[Continued on next page]

WO 02/055993 A2



Eurasian patent (AM, AZ, BY, KG, KZ, MD, RU, TJ, TM), European patent (AT, BE, CH, CY, DE, DK, ES, FI, FR, GB, GR, IE, IT, LU, MC, NL, PT, SE, TR), OAPI patent (BF, BJ, CF, CG, CI, CM, GA, GN, GQ, GW, ML, MR, NE, SN, TD, TG).

**Declarations under Rule 4.17:**

- *as to applicant's entitlement to apply for and be granted a patent (Rule 4.17(ii)) for the following designations AE, AG, AL, AM, AT, AU, AZ, BA, BB, BG, BR, BY, BZ, CA, CH, CN, CO, CR, CU, CZ, DE, DK, DM, DZ, EC, EE, ES, FI, GB, GD, GE, GH, GM, HR, HU, ID, IL, IN, IS, JP, KE, KG, KP, KR, KZ, LC, LK, LR, LS, LT, LU, LV, MA, MD, MG, MK, MN, MW, MX, MZ, NO, NZ, OM, PH, PL, PT, RO, RU, SD, SE, SG, SI, SK, SL, TJ, TM, TN, TR, TT, TZ, UA, UG, UZ, VN, YU, ZA, ZM, ZW, ARIPO patent (GH, GM, KE, LS, MW, MZ, SD, SL, SZ, TZ, UG, ZM, ZW), Eurasian patent (AM, AZ, BY, KG, KZ, MD, RU, TJ, TM), European patent (AT, BE, CH, CY, DE, DK, ES, FI, FR, GB, GR, IE, IT, LU, MC, NL, PT, SE, TR), OAPI patent (BF, BJ, CF, CG, CI, CM, GA, GN, GQ, GW, ML, MR, NE, SN, TD, TG)*
- *of inventorship (Rule 4.17(iv)) for US only*

**Published:**

- *without international search report and to be republished upon receipt of that report*

*For two-letter codes and other abbreviations, refer to the "Guidance Notes on Codes and Abbreviations" appearing at the beginning of each regular issue of the PCT Gazette.*

---

potential within the ideally polarizable region. Because of potential induced changes in the shape of the SPR curve, we account for the full curve rather than simply the shift in the resonance minimum. The hybridization of complementary strands of DNA is the underlying principle of all microarray-based techniques for analysis of DNA variation. In this paper, we study how probe immobilization at surfaces, specifically probe density, influences the kinetics of target capture using surface plasmon resonance (SPR) spectroscopy, an in-situ label-free optical method. Probe density is controlled by varying immobilization conditions, including solution ionic strength, interfacial electrostatic potential, and whether duplex or single stranded oligonucleotides are used. Independent of which probe immobilization strategy is used, we find that DNA films of equal probe density exhibit reproducible efficiencies and reproducible kinetics for probe/target hybridization. However, hybridization depends strongly on probe density in both the efficiency of duplex formation and the kinetics of target capture. We propose that probe density effects may account for observed variation in target capture rates which have previously been attributed to thermodynamic effects.

TITLE OF THE INVENTION  
USE OF ELECTROSTATIC FIELDS TO ENHANCE SURFACE  
PLASMON RESONANCE SPECTROSCOPY

5 CROSS REFERENCE TO RELATED APPLICATIONS

This application claims priority from U.S Provisional Patent Application Ser. No. 60/261,504, filed January 12, 2001, and U.S. Provisional Patent Application Ser. No. 60/340,145, filed December 14, 2001, both of which are incorporated in their entirety herein.

10 STATEMENT REGARDING FEDERALLY SPONSORED RESEARCH OR  
DEVELOPMENT

This invention was made with Government Support  
15 under Contract Numbers CHE 9709347 and DBI-0096731 awarded by the National Science Foundation. The Government has certain rights in this invention.

20 BACKGROUND OF THE INVENTION

Many qualitative and quantitative assays of biomolecular interactions are based on detecting the binding of solution phase targets with surface bound probes. Success of such assays depends on many parameters of the probe-modified surface (probe density, attachment chemistry, characteristics of the attachment linker, components introduced to reduce non-specific binding, interface surface charge density) as well as solution conditions such as ionic strength. For example, increasing research efforts are directed towards the detection of nucleic acid interactions with immobilized oligonucleotide probes for DNA microarray applications <sup>1,2</sup>. Limitations of most current technologies include

complex DNA immobilization procedures, the need for fluorescence or other labeling, and slow hybridization kinetics that require long incubation times. In addition, those experimental conditions that optimize 5 DNA duplex formation often also reduce the stringency of hybridization. That is, for oligonucleotides that are sufficiently long to distinguish a particular sequence in the presence of unrelated DNA, a mismatched base pair has only a marginal effect on the stability of the 10 duplex.<sup>3</sup> In DNA microarray and other applications, mismatched hybrids lead to "false positives" which can a limiting factor for successful single nucleotide polymorphism (SNP) detection or mutation detection.

The use of an electric field to easily control the 15 electrostatic forces on surface-immobilized polyelectrolytes such as DNA is a means for improving the speed and stringency of biomolecular interactions at interfaces. Control of electrostatic forces can therefore improve assays that rely on biomolecular 20 interactions. In this invention, *in-situ* optical surface plasmon resonance spectroscopy (SPR) is used to monitor hybridization kinetics for unlabeled DNA in tethered monolayer nucleic acid films on gold in the presence of an applied electrostatic field. These 25 experiments can also be performed over a wide range of temperatures, for example 10-80 degrees Celsius.

#### BRIEF SUMMARY OF THE INVENTION

30 *In-situ* optical surface plasmon resonance spectroscopy (SPR) can be used to monitor hybridization kinetics for unlabeled DNA in tethered monolayer nucleic

acid films on gold in the presence of an applied electrostatic field. The DC field can enhance or retard hybridization and can also denature surface-immobilized DNA duplexes. Discrimination between matched and 5 mismatched hybrids is achieved by simple adjustment of the electrode potential. Although the electric field at the interface is extremely large, the tethered ssDNA thiol probes remain bound and can be reused for subsequent hybridization reactions without loss of 10 efficiency. Only capacitive charging currents are drawn; redox reactions are avoided by maintaining the gold electrode potential within the ideally polarizable region. Because of potential induced changes in the shape of the SPR curve, we account for the full curve 15 rather than simply the shift in the resonance minimum.

The hybridization of complementary strands of DNA is the underlying principle of all microarray-based techniques for analysis of DNA variation and many other applications. In this invention, we also discovered how 20 probe immobilization at surfaces, specifically probe density, influences the kinetics of target capture using surface plasmon resonance (SPR) spectroscopy, an in-situ label-free optical method. Probe density is controlled by varying immobilization conditions, including solution 25 ionic strength, and whether duplex or single stranded oligonucleotides are used. In addition, electrostatic fields can be used for controlling the extent of immobilization or attachment of biomolecules, such as thiol-derivatized oligonucleotides. Independent of which 30 probe immobilization strategy is used, we find that DNA films of equal probe density exhibit reproducible efficiencies and reproducible kinetics for probe/target

hybridization. However, hybridization depends strongly on probe density in both the efficiency of duplex formation and the kinetics of target capture. Probe density effects may account for observed variations in  
5 target capture rate and capture efficiency that have previously been attributed to thermodynamic effects.

#### BRIEF DESCRIPTION OF THE FIGURES

10 Figure 1 shows (A) potential induced changes in the shape of the SPR curve for bare gold (reflectance vs. angle of incidence) and (B) the impact of potential on optical dielectric constants.

15 Figure 2 compares kinetics of hybridization at open circuit (squares) and under electrochemical control at applied potentials of +300 mV (circles) and -300mV (triangles).

20 Figure 3 shows discrimination between fully complementary hybrid and two base-pair mismatch hybrid by electric field induced denaturation on the same surface.

Figure 4 shows the extent of non-specific binding  
25 for matched and unmatched (control) DNA.

Figure 5 contains representative data for immobilization kinetics of ssDNA-C<sub>6</sub>-SH (closed squares) and dsDNA-C<sub>6</sub>-SH (open circles) from 1  $\mu$ M DNA solutions in  
30 1 M KH<sub>2</sub>PO<sub>4</sub>.

Figure 6 contains the comparison of probe immobilization kinetics as a function of ionic strength formed from solutions containing (A) 1  $\mu\text{M}$  dsDNA-C<sub>6</sub>-SH and (B) 1  $\mu\text{M}$  ssDNA-C<sub>6</sub>-SH.

5

Figure 7 shows the immobilization kinetics from 1  $\mu\text{M}$  ssDNA-C<sub>6</sub>-SH solutions in 1 M NaCl in the presence and absence of an applied potential. For potential-assisted immobilization, the potential is held at +0.3V vs. 10 Ag/AgCl (triangles). The unassisted immobilization is at open circuit (open circles).

Figure 8 shows target hybridization kinetics as a function of probe density. The probe density, 15 determined by SPR, varies from  $2 \times 10^{12}$  to  $12 \times 10^{12}$  molecules/cm<sup>2</sup>. Heating of the probe film prior to hybridization increases the hybridization efficiency. All runs are 1  $\mu\text{M}$  target in 1 M NaCl with TE buffer.

20 Figure 9 shows hybridization kinetics as a function of probe density. The same data as in Figure 8; however, the data are now normalized. The data show distinct behavior that correlates with two regimes for probe density: Low ( $<3 \times 10^{12}$  moelcules/cm<sup>2</sup>), and High ( $>5 \times 10^{12}$  25 molecules/cm<sup>2</sup>).

Figure 10 shows the comparison of probe/target capture kinetics for probe films formed by different immobilization strategies. Hybridization kinetics are 30 shown for two low probe density films,  $\sim 3 \times 10^{12}$  molecules/cm<sup>2</sup> (circles) and two high probe density films,  $\sim 1.2 \times 10^{13}$  molecules/cm<sup>2</sup> (triangles). Probe films at low

density, formed either from ssDNA-C<sub>6</sub>-SH immobilization (filled circles) or via dsDNA-C<sub>6</sub>-SH immobilization (open circles) show comparable kinetics and overall efficiency of capture. Similarly, probe films formed via 5 immobilization of ssDNA-C<sub>6</sub>-SH under electrostatic conditions of +0.3V (open triangles) or via incubation overnight at open circuit (filled triangles) are indistinguishable. All hybridization kinetics obtained under the same conditions of 1  $\mu$ M target in 1 M NaCl with 10 TE buffer.

Figure 11 shows an example of a strategy for forming probe films of desired density using pulsed potentials. For example, to prepare a probe density of  $5 \times 10^{12}$  molecules/ cm<sup>2</sup>, three sequential pulses at +400 mV (each pulse 5-10 sec) is needed. The rest potential (between attractive pulses) was set to -300 mV (repulsive). For this repulsive potential, little if any immobilization is observed. Solutions used for these electrostatically 20 assisted immobilization experiments contain 1  $\mu$ M concentration of the desired probe ssDNA-C<sub>6</sub>-SH (SEQ ID NO 1).

#### DETAILED DESCRIPTION OF THE INVENTION

25

The monolayer DNA thiol films used in this work are tethered directly to the SPR metal sensor surface through a gold-thiol covalent attachment. Therefore, the immobilized DNA hybrids are exposed to a field 30 gradient at the metal/electrolyte interface on the order of  $10^9$  V/m. We show that this field can be used, in a reversible manner, to increase or decrease the rate of

oligonucleotide hybridization. In addition, we show that a repulsive potential preferentially denatures mismatched DNA hybrids within a few minutes while leaving the fully complementary hybrids largely intact.

5 This sequence selectivity in hybrid denaturation imparts an extremely high stringency for assaying DNA interactions and represents an extremely simple, novel method for mutation detection based purely on electrostatic charging effects. Finally, electrostatic

10 fields can be used for controlling the extent of immobilization or attachment of biomolecules, such as thiol-derivatized oligonucleotides. We propose that this method of patterning (selectively assisting or preventing immobilization in a specific region of the

15 surface) can be used not only on bare gold SPR sensors but also on chemically modified surfaces.

This work is in contrast with the "electronic denaturation" of DNA hybrids reported by Heller and coworkers <sup>4</sup> in which an electric current is reported to

20 denature fluorescent-labeled DNA oligonucleotides immobilized in a gel. In that case, denaturation is likely to arise through a complex mechanism, potentially involving Joule heating within the gel, formation of hydroxyl ion or radical intermediates or other current-

25 induced phenomena. Direct electric field denaturation cannot be the mechanism as the potential gradient in the gel, on the order of a few hundred volts per meter, is insufficient to destabilize the hybrid.

Despite the extremely large field strengths at the

30 electrochemical interfaces used here, the current is limited to capacitive, non-Faradaic charging current. Redox reactions are avoided by maintaining the gold

electrode potential within the ideally polarizable region. The tethered ssDNA thiol probes remain bound and can be reused for subsequent hybridization reactions without loss of efficiency. The robustness of these monolayer films is not surprising given the well-known extensive use of alkanethiol self-assembled monolayer films in a wide range of electrochemical applications. The specific DNA thiol films used here have been extensively characterized in previous work by various techniques,<sup>5</sup> including neutron scattering<sup>6</sup> and SPR surface melting experiments<sup>7</sup> and are known to be robust and reusable in non-electrochemical experiments even after heating to 75 ° C. Previous *in-situ* SPR experiments confirm that the thermal stability of dsDNA on these surfaces is analogous to that observed in free solution<sup>7,8</sup>.

This work is distinguished by the use of label-free SPR detection of hybridization and denaturation achieved by monitoring gain or loss of DNA at the interface in the presence of applied electrochemical field. Although a wide body of literature describes the application of SPR to study the interactions of biologically active species with surfaces, films and biomaterials, including DNA hybridization,<sup>5-7,9</sup> relatively few applications of electrochemical SPR have appeared in the literature. None of these previous electrochemical studies have used capacitive, non-Faradaic charging of the sensor interface to control biomaterial interactions. The combination of SPR with electrochemistry has been limited to cases where electrochemical currents associated with oxidation/reduction reactions at the metal SPR substrate are monitored simultaneously.

Previous work includes investigations of immobilized protein redox reactions<sup>10,11</sup>, selective desorption of monolayer films<sup>12</sup>, reversible doping of organic conducting polymer films<sup>13</sup>, and electrochemical release 5 of surface bound ligands<sup>14</sup>.

It is well known that the application of an interfacial electric field alters the ionic double layer at the metal/electrolyte interface. It is well known that a change in the concentration of ions in the vicinity of 10 DNA or other biopolymers can cause changes in conformational structure and binding affinity. At high ionic strengths (a condition which favors hybridization of DNA, for example), the Debye screening length is very short on the order of a few Angstrom. Therefore, the 15 effect of the electrostatic field might be expected to be completely screened at distances comparable with the length of DNA strands which are immobilized on the surface of gold SPR sensor used in these experiments. Nevertheless, we find numerous strong effects of the 20 applied fields which act to enhance surface plasmon resonance spectroscopy.

In order to enhance surface plasmon resonance spectroscopy with the use of electrostatic fields it is necessary to detect or have knowledge of the full SPR 25 curve. This is because application of an interfacial electric field alters the surface electron distribution and therefore the optical properties of the metal. For bare metal surfaces, this effect has been measured by a number of different surface optical techniques including 30 SPR, electroreflectance, second harmonic generation and ellipsometry. In SPR, potential-induced optical changes lead to substantial alteration in the shape of the

reflectance spectrum; therefore, we account for the full SPR curve rather than simply the shift in the resonance minimum.

With detection or knowledge of how the SPR curve 5 behaves in the presence of electrostatic fields (that is, acquisition and analysis of the SPR curve in the way described here), it is possible to measure and detect quantitatively various chemical and physical changes at the surface of the SPR sensor such as the attachment, 10 hybridization, and binding of solution phase biomolecules. The control of the electrostatic field at the interface combined with the *in-situ* label-free detection of the SPR method, provides advantages of speed, selectivity and sensitivity over other methods.

In this work, all SPR data are obtained from reflectance measurements from a *single* region of the gold 15 SPR sensor surface and the same DNA probe surface is regenerated and re-used for sequential experiments. However, multiple experiments can be carried out 20 simultaneously (parallel sensing) using a different implementation of SPR where light reflected from many different regions of the sensor is monitored. A number of designs for SPR multichannel sensing have appeared in the literature. What distinguishes our approach from the 25 current methods is that we propose to obtain locally resolved SPR curves rather than simply monitoring the reflected intensity from the surface regions of interest. This capability takes this instrument beyond just qualitative comparisons between binding kinetics obtained 30 from each channel to quantitative measurements of coverage and kinetics.

The term "locally resolved SPR curve" or "spatially resolved SPR curve" is defined as having two parts. 1) "locally resolved" or "spatially resolved" refers to the fact that the measurement of the surface plasmon resonance condition can be obtained for one or more spatially distinct regions of the sensor surface ranging in size from a few square micrometers to millimeter square or larger depending on the area probed (by illumination for example) and the dimensions of the detector. 2). "SPR curve" refers to the variation of the surface plasmon resonance condition as a function of wavelength, wavevector or angle of incidence. In some examples, this is referred to as a full SPR reflectance dip.

There are at least two ways to obtain spatially resolved SPR curves for microarray applications. The first involves spatially resolved CCD (charge-coupled device) imaging of the reflectance from the surface of the microarray as a function of angle of incidence array at fixed frequency. This approach requires the mechanical motion of rotation stages. The other approach keeps the angle of incidence fixed (no moving parts) and uses a tunable light source which can be swept rapidly over a wide range of wavelengths. Only one wavelength will couple fully with the SP oscillation and a spectral analysis of the reflected light will show an absorption dip at this resonant wavelength. An acousto-optic tunable filter (AOTF) or other device (e.g., LCTF, liquid crystal tunable filter) will be used to modulate the frequency of the light over a large enough wavelength range so the full SPR reflectance dip as a function of wavelength can be measured without the need for a

monochromator. This wavelength scanning approach has been demonstrated for simple non-imaging SPR and, in that case, differential wavelength scanning is 2-orders of magnitude more sensitive than conventional angular 5 scanning for tracking the SPR minimum reflectance resonance condition.

We have used electrostatic charging to increase and decrease the rate of target DNA adsorption onto a probe surface. Under electrostatic assistance, the initial rate 10 of target adsorption is greater than for passive hybridization. This effect is especially pronounced for the mismatch target. Interestingly, the steady state coverage reached by electrostatic assistance never exceeds that for passive hybridization. This in agreement 15 with previous work<sup>7</sup>, which showed that, for these two-component DNA films, the mercaptohexanol component is a diluent that serves to block non-specific adsorption of DNA.

Application of a repulsive potential preferentially 20 denatures mismatched hybrids within a few minutes or seconds, leaving the fully complementary 25-mer hybrids largely intact even after many hours. This sequence selectivity in hybrid denaturation imparts an extremely high stringency for assaying DNA interactions and 25 represents a novel, yet extremely simple, method for mutation detection based purely on electrostatic charging effects. The electrostatically assisted SPR methods outlined here are also applicable in an array format currently under development in our laboratory.

30 In contrast with previous "electronic denaturation" of DNA hybrids reported previously by Heller and coworkers,<sup>4</sup> here the DNA is immobilized directly at the

metal/electrolyte interface and therefore is exposed to a field gradient on the order of  $10^9$  V/m. This electrostatic field is sufficient to induce denaturation of the hybrids. Because no Faradaic current flows, the 5 ssDNA probes remain covalently bound to the gold and are stable to prolonged exposures at these electrode potentials. Finally, the simple planar geometry of our SPR substrate and the use of DNA monolayer films of controlled coverage means that electric field induced 10 denaturing at these simple interfaces are likely to be theoretically tractable.

We use surface plasmon resonance spectroscopy (SPR) to monitor the kinetics of probe attachment as well as the process of target capture. This technique, which does 15 not require fluorescence probes or other labels, has been used previously in our laboratory to study the kinetics and thermodynamics of DNA monolayer films <sup>7,8,15</sup>. Attachment of DNA probe to solid supports can be achieved by covalent or non-covalent attachment strategies. Here, 20 we used covalent attachment based on gold/thiol bond formation a method shown previously to result in robust and reusable DNA probe films <sup>6,7,16</sup>. In addition to the thiol modified 25-mer DNA oligonucleotide component, the self-assembled monolayer film also contains 25 mercaptohexanol. For the resulting films, non-specific adsorption of DNA is negligible as reported previously <sup>7,8,15</sup>.

Varying the amount of time that the solid support is exposed to the DNA-thiol solution can control the probe 30 density of the film, however, other strategies can be used. In this development, we use several additional approaches including varying the solution ionic strength

and applying an attractive electrostatic field at the interface to assist in the immobilization of negatively charged ssDNA-C<sub>6</sub>-SH. Also, we compare the immobilization of duplex DNA-C<sub>6</sub>-SH, which has a thiol linker on one of 5 the oligonucleotide strands in contrast to ssDNA-C<sub>6</sub>-SH immobilization under the same solution conditions. While the immobilization of ssDNA is more commonly used, some researchers have used duplexes. One might expect that, after denaturation of the duplex film, the probe density 10 may be more optimum for hybridization, compared with immobilization of ssDNA that could lead to films that are too tightly packed for efficient hybridization.

We find probe density to be a controlling factor for the efficiency of target capture as well as for the 15 kinetics of the target/probe hybridization. In the lowest probe density regimes, essentially 100% of probes can be hybridized and the kinetics of binding follow Langmuir-like kinetics, whereas at high probe density the efficiencies drop to about 10% and the kinetics are also 20 slower. The high efficiencies achieved here are in contrast to the typically low efficiencies of hybridization found for many DNA microarrays, where sensitive fluorescence detection is used. For example, Forman and coworkers <sup>17</sup> report saturating adsorption 25 densities at perfect match probe sites to be < 10% of the probe density.

All quantitative measurements of DNA surface density for probe oligonucleotides and bound targets are obtained using surface plasmon resonance spectroscopy. This work 30 is characterized by highly reproducible data: independent of which immobilization strategy is used, we find that DNA films of equal probe density exhibit reproducible

efficiencies and reproducible kinetics for probe/target hybridization.

Surface density of the probe strand is a key factor that determines the extent to which immobilized probes  
5 are able to capture solution phase targets. In low probe density regimes, essentially 100% of probes can be hybridized and the kinetics of binding follow comparatively faster kinetics whereas at high probe density the efficiencies drop and the kinetics are  
10 slower. In both cases, however, the hybridization isotherms remain complex and cannot be fit with simple kinetic models. Various strategies can be used to tailor immobilization and control the surface probe density. For all strategies used, the functionality of  
15 the film remains the same when compared at the same probe density. Most importantly, there is a strong dependence on probe density for both the efficiency of duplex formation and the kinetics of target capture.

The technique developed is also applicable for  
20 quantifying the amount of target present in the sample. This assay would be conducted by running a series of known concentrations of a given target and drawing a calibration curve against which the unknown sample would be compared.

25 In this invention, analysis of a locally resolved SPR curve is used to determine the average surface coverage even in the presence of an applied electrostatic field. These measurements of surface coverage are used to determine probe target binding at  
30 the SPR sensor surface. Finally, a pattern of probe target binding can be obtained by monitoring the change in coverage or binding as a function of time, applied

electrode voltage or some other experimental parameter such as solution concentration, pH, ionic strength, temperature etc. More than one experimental parameter can be varied simultaneously if desired. For 5 quantitative determination of surface coverage in the presence of an applied field, analysis of the full SPR curve is performed. Alternatively, a portion of the SPR curve may be used in some applications.

The pattern of probe target binding studied in this 10 invention is the kinetics of DNA hybridization (capture of solution phase targets by an immobilized DNA probe) or the kinetics of duplex denaturation (loss of DNA originally hybridized to an immobilized DNA probe). Although most of the detailed descriptions in this 15 invention are focused on oligonucleotides, comparable techniques can be used for a wide range of biological targets including proteins, polypeptides, whole cells and parts of cells since SPR is a general method that is applicable to all of these biological targets. 20 Electrostatically assisted SPR can be used for any biological target that contains a charged moiety.

The following examples are intended to further illustrate, not limit, the invention.

25

#### Example 1: Instrumentation

The SPR optical instrumentation used for these experiments has been described previously <sup>7,18,19</sup>. For SPR 30 spectroscopy in the so-called Kretschmann geometry, light illuminates the interface from the back of the sensor surface rather than a light beam sent through the bulk

liquid sample. The components of this instrument are 1) a light source, such a laser, LED (light emitting diode) or lamp, with emission at a select wavelength or range of wavelengths, for example visible wavelengths or infrared, 5 2) optics for collimating or focusing the light onto the SPR sensor surface 3) a polarizer for selecting the polarization of light, 4) a prism (such as an equilateral or hemicylindrical or other shape) or other optic onto which a thin metal film has been evaporated to 10 create the SPR sensor surface. The metal film is typically about 500 Å in thickness and can consist of gold, silver, copper or any alloy or semiconductor material with sufficient density free electron carriers to support a plasmon oscillation, 5) a method of coupling 15 the light to surface plasmon, for example through the use of a prism coupler 6) a means of detecting the intensity of the reflected light, for example a photodiode, linear photodiode array or CCD camera. 7) a means of controlling and varying the angle of incidence of the light beam on 20 to the prism coupler and 8) means of bringing a liquid or gaseous sample in contact with the sensor surface, for example a fluid cell made of Teflon, plastic or glass and 9) fluid handling equipment for example microfluidic components can also be used. Finally, for SPR biosensor 25 applications, a method is needed for immobilizing or attaching the probe compounds to the surface either directly or through a series of intermediate molecular or polymeric connection, for example self assembled monolayer formation, attachment to polysaccharides 30 matrices.

An example of instrumental design for an angular scanning apparatus is the following. For angular

scanning surface plasmon resonance spectroscopy measurements, for example in the study of self assembly kinetics of monolayer films, (23) the apparatus utilized a He-Ne laser (Uniphase, 632.8 nm output, 2 mW), as the 5 light source and a photodiode (Thor Labs, model PDA50) to detect the reflected light intensity. The output of the He-Ne laser is set for p-polarized incident light with respect to the plane of incidence on the gold 10 surface using a polarizing cube (Precision Optics) and various optics are used to focus light onto the prism. The prism is directly attached to the sample cell which consists of a custom built PTFE liquid cell with Kalrez o-ring, PTFE-coated thermocouple probe and fluid handling ports. The cell/prism assembly is mounted at the center 15 of motorized θ/2θ goniometer (Aerotech), which is used to control the light incidence angle on the prism. Equilateral or hemispherical prisms of different materials are used, for example BK7, SF10 and SF14 (Schott Glass). Higher refractive index is desirable as 20 this moves the angle of the reflectance minimum to lower angle making it possible to measure a larger portion of the full reflectance curve.

The motorized goniometer is controlled by a PC through a goniometer interface (Aerotech). All optical 25 and temperature data are collected through an analogue to digital data acquisition board controlled by LabView for Windows™. The analysis software for the SPR reflectance curves was adapted and optimized for Matlab for Windows™ from a code originally written by J. D. Swalen (IBM 30 Almaden).

The accuracy of the measurement depends on several factors, including temperature, alignment, and laser

stability. We monitored the temperature of solutions in the sample cell throughout our experiments and used the temperature corrected refractive indices in all of our calculations. At the beginning of each experiment, the  
5 laser beam is aligned to within 0.005° of the prism face. The goniometer moves the prism and photodiode with a resolution of <0.001°. After several days of scanning, the maximum change in alignment was 0.005°. The maximum change in laser power for each measurement was 0.20% rms,  
10 and the laser signal was renormalized for each measurement. The calculated accuracy and precision is <0.8 Å for our measurements of alkanethiol monolayer film thickness. (23)

Alternative designs are also possible including  
15 instrument designs with use fiberoptic coupling for SPR or instruments for which the excitation laser beam passes through the sample solution.

The electrochemical experiments use a potentiostat (EG&G 263A) to control the potential of a standard three-electrode cell, as described previously.<sup>13</sup> The cell employs the gold SPR substrate as the working electrode, a platinum counter electrode in the bulk solution and an Ag/AgCl reference electrode placed in a remote reservoir that is connected to the SPR cell through a salt bridge  
25 (Vycor plug).

In this invention, a potential is applied to the gold SPR surface (working electrode) and SPR data is collected at the same time. Alternatively, SPR data could be collected before and after application of the  
30 potential. For electrostatic charging (the preferred technique), the applied electrode potential is maintained within the ideally polarizable region (IPR), thus only

capacitive non-Faradaic charging occurs and electrochemical redox reactions are avoided. Alternatively, for potentials outside of the IPR, Faradaic currents are present. The IPR can be determined 5 from current vs voltage scans. We use the terms applied potential or applied voltage interchangeably to refer to both the condition where with Faradaic or non-Faradaic currents are present.

Preparation of the SPR gold substrate and subsequent 10 self-assembly of the ssDNA monolayer film was carried out as described previously <sup>7</sup> and described below. Prior to assembly of the sample cell, preparation of the SPR sensor surface is achieved by coating the surface of the prism (or a slide of appropriate refractive index) with 15 a thin film of gold. This is achieved by electron beam evaporation of ~ 10 Å of Cr followed by ~500 Å gold (99.99%) (1-2 Å/s) at a base pressure of  $7 \times 10^{-7}$  torr. The glass substrates were previously cleaned by 15 minute exposure to 3:1 H<sub>2</sub>SO<sub>4</sub>-H<sub>2</sub>O<sub>2</sub> (piranha solution) at 70° C 20 followed by rinsing in nanopure (18 MΩ) water and baking overnight in a 100°C oven. The gold films can be reused, even after chemical attachment of covalently bound monolayer films. Before each new set of experiments, the gold substrate is exposed to freshly made (~50° C) H<sub>2</sub>SO<sub>4</sub>- 25 H<sub>2</sub>O<sub>2</sub> solution for about 2-10 minutes and rinsed with copious quantities of nanopure water. This treatment was repeated until nanopure water was observed to fully wet the gold surface.

Once the gold substrate is prepared, the desired 30 probe materials are immobilized while monitoring with in-situ SPR. Procedures for immobilizing monolayer films of DNA and other molecules onto the gold SPR

substrate have been published by numerous authors. Many techniques exploit self assembled monolayers based on alkanethiol/gold covalent attachment chemistry. For these experiments, the immobilized monolayer films (DNA probe films) are a two-component film, which consists of a 25-mer single-stranded DNA functionalized with a pendant  $(\text{CH}_2)_6\text{SH}$  at the 5' position and a diluent mercaptohexanol.<sup>7,8,15,16,20</sup> (SEQ ID NO 1) The mercaptohexanol component serves to block non-specific adsorption of DNA.

**Example 2: Probe immobilization and hybridization experiments**

**Oligodeoxyribonucleotide Sequences**

All oligonucleotides, Table 1, were obtained from commercial vendors with purification by HPLC. For example, thiol functionalized DNA oligonucleotides were obtained from Integrated DNA Technologies or Synthegen; unfunctionalized DNA oligonucleotide targets were obtained from Alpha DNA.

**Preparation of Solutions**

All solutions were prepared using purified water (18 M Ohm  $\text{cm}^{-1}$  resistance, Barnstead E-pure). All probe, target and duplex solutions (1  $\mu\text{M}$ ) were prepared at the specified salt concentration. Electrolyte solutions were  $\text{KH}_2\text{PO}_4$  (1 M, Aldrich) and  $\text{NaCl}$  (1M, 0.1 M, 0.05 M, Fisher) with all  $\text{NaCl}$  solutions containing TE Buffer (10 mM Tris Buffer (pH 7.2) and 1 mM EDTA) (Sigma). Mercaptohexanol (Aldrich) was prepared as a 1 mM solution in water.

Immobilization Procedure (in the absence of electrostatic fields)

Before all immobilization experiments, the gold substrate was cleaned with piranha solution (7:3 mixture of H<sub>2</sub>SO<sub>4</sub> and H<sub>2</sub>O<sub>2</sub>). For each DNA experiment, the gold SPR substrate was exposed to DNA solution for >10 hours unless otherwise stated. The ssDNA-C<sub>6</sub>-SH probe film was treated with 1 mM mercaptohexanol solution for 1-2 hours. For the case of duplex immobilization, the ds-DNA-C<sub>6</sub>-SH film is immobilized as a pre-hybridized probe (ssDNA-C<sub>6</sub>-SH) and target (ssDNA) combination. Before the exposure of the target to the dsDNA-C<sub>6</sub>-SH (SEQ ID NO 2 and SEQ ID NO 3) film the duplex was denatured to create a ssDNA probe surface. No more than half the mass of the immobilized duplex film is lost during heating to 80°C, consistent with the removal of the target strand only; no thiol DNA is lost upon heating <sup>7</sup>. For both types of prepared probe surfaces, a control experiment was done (using a non complementary target solution) to ensure that no non-specific binding occurred.

Denaturation

For most experiments, repeated measurements were performed on the same DNA film requiring regeneration of the ssDNA probe film. This was achieved by the denaturation of the surface duplex by rinsing with hot water.

**Example 3: Analysis of SPR results in the presence of an applied electrostatic field**

Analysis of SPR curves for quantitative  
5 determination of surface coverage of DNA or other  
biomolecules-General

In general, surface coverage at the SPR sensor and consequently, the extent of probe target binding, can be determined from analysis of SPR reflectance data. For 10 quantitative determination of coverage, analysis of the full SPR curve is preferred. Alternatively, a portion of the curve can also be monitored.

The two-color SPR apparatus set-up and procedure for analysis of measurements have been described previously, 15<sup>18,19</sup> as have details of how quantitative measurements of coverage are extracted from raw SPR reflectance data. Briefly, the SPR reflectance data were analyzed by fitting the data to a multilayer Fresnel model to extract the thickness and dielectric constant of the unknown DNA 20 layer. The resulting best-fit parameters are converted to coverage of DNA (in molecules/cm<sup>2</sup>) as outlined previously<sup>6,7,16</sup>. Hybridization efficiencies are calculated as the fraction of hybridized target coverage divided by the immobilized probe coverage. As in previous work, these 25 calculations assumed an equivalent SPR response per unit coverage for single stranded DNA oligonucleotides at the surface of the SPR substrate regardless of whether the DNA consisted of surface-immobilized probe molecules or target DNA undergoing hybridization at the surface.  
30 Good agreement has been reported<sup>5,21,22</sup> between our SPR

measurements and radiolabeling experiments and quantitation by other methods such as electrochemistry.

SPR detection in the presence of an applied  
5 electrochemical field.

The same type of analysis as described in the previous section of Example 3 can be used to determine coverage or probe target binding in the presence of an applied electrostatic field. However, since the applied  
10 electrostatic field can alter the shape of SPR curve, the full SPR curve should be considered in the analysis. These potential induced changes in the SPR must be distinguished from changes that arise due of variation in the coverage.

15 In this example we establish the potential dependence of the optical properties for bare gold SPR substrates and substrates coated with monolayer films in the absence of any binding or coverage change. This information, Figure 1, is then used in the data analysis.  
20 That is, SPR curves are fit with a contribution that accounts for the potential induced changes in the optical properties of the sensor and another contribution that accounts for changes in biomolecular binding. Potential induced changes in the shape of the SPR curve  
25 (reflectance vs angle of incidence) for bare gold are shown in Fig. 1A for a series of applied potentials (0, 200, 400 and 600 mV). The alterations in shape can be accounted for by changes in the optical constants of the gold substrate, Fig. 1B, in excellent agreement with the  
30 results from previous work.<sup>23</sup> Here, the complex dielectric constant of the gold as a function of applied potential was calculated from fitting the SPR reflectance

data assuming that only the outermost 2 Å of the gold are affected by the electric field. In agreement with previous optical studies of electrochemical interfaces, we find a strong potential dependence at potentials 5 positive of the potential of zero charge, (PZC), and a negligible effect at potentials negative of the PZC (approximately +100 mV). As expected, the charging behavior depends on the nature of the electrolyte. Detailed studies in various electrolytes (data not shown) 10 show that the strongest potential dependence at positive charging is observed for systems with the most negative value of the PZC. The series of electrolytes studied, our results are consistent with the trend of PZC(chloride) < PZC(phosphate) ~ PZC(sulfate) < 15 PZC(perchlorate), in agreement with previous electrochemical determinations of the PZC. In chloride solutions which exhibit the lowest PZC, the potential dependence at the positive charging is about 20% larger than the magnitude shown in Fig. 1B.

20 The presence of a self-assembled monolayer film suppresses the potential dependence of the SPR response. For example, for a complete, well-packed monolayer of dodecanethiol the potential dependence is essentially eliminated. For the two-component ssDNA thiol/ 25 mercaptohexanol monolayer film used in this work, the SPR response potential dependence is suppressed to approximately 10% of that of bare gold in the same electrolyte solution.

**Example 4: Hybridization in the presence of electrostatic fields.**

In this section, we examine the effect of electrostatic charging on target/probe hybridization.

Hybridization was achieved by exposing the immobilized ssDNA probe surface to 1  $\mu\text{M}$  target DNA solution in 1 M NaCl for up to a total of 14 hours for passive hybridization and up to 5 hours for electric field assisted hybridization. For all hybridization experiments performed under electrochemical control, the surface was first exposed to target DNA solution at open circuit. After a short time, less than 60 s, the desired potential (for example, +300 mV for assisted hybridization or -300 mV for electrostatic denaturation, see Example 5) was applied immediately after sweeping to the desired potential from the potential of zero charge (PZC) at a rate of 50 mV  $\text{s}^{-1}$ . For electric field assisted denaturation experiments and electric field assisted hybridization, the applied field could be maintained for many hours without deterioration of selectivity or sensitivity.

All data presented in Figures 2-4 are obtained on the same regenerated probe surface however consistent results (within the noise) are seen on different gold/DNA thiol interfaces. Hot water (90 °C) rinses were used to regenerate the ssDNA probe surface for sequential experiments. All potentials are reported with respect to an Ag/AgCl reference electrode. For all electrochemically-assisted experiments, the applied potential remains within the ideally polarizable region (IPR) so as to avoid any oxidation/reduction reactions at the electrode surface.

Fig. 2 shows the data for electrostatically controlled experiments compared with hybridization under passive, open circuit, conditions for a fully complementary target (left panel) and a partially mismatched target (right panel). The ordinate is given as percentage of the steady-state hybridization. That is, the DNA coverage is calculated from analysis of the SPR reflectance curves. The progress of hybridization is shown as the percent of the duplex DNA surface coverage relative to the steady state coverage achieved after ~14 hours of hybridization at open circuit.

Application of an attractive potential (+300 mV) increases the rate of duplex formation for both the matched and mismatched target DNA compared with passive hybridization (open circuit or OC). Interestingly, the hybridization enhancement is much more pronounced for the mismatched target. (I.e., the difference between the extent of hybridization at positive charging relative to open circuit is much larger for the mismatched target.) The extent of hybridization with field assistance is never larger than when hybridization is carried out with overnight incubation at open circuit. Application of a repulsive potential (-300 mV) immediately halts hybridization.

Control experiments with the non-complementary DNA oligomer show that non-specific binding is negligible even in the presence of an applied electrostatic field of + 300 mV, see Fig. 4. These results are in agreement with previous work under open circuit conditions<sup>7,8,16</sup> which showed that the mercaptohexanol component appears to help block non-specific adsorption of DNA. As with previous work, the kinetics of

hybridization for a specific sequence and probe density are reproducible within the noise for other gold substrates.<sup>7,8,16</sup>

We have reported previously that, at open circuit,  
5 the kinetics of hybridization provide a means of discriminating against mismatched DNA duplex formation.  
<sup>8</sup> That is, the kinetics of hybridization for matched duplexes (filled squares in Fig. 2) are clearly distinct from those of mismatched DNA hybridization (unfilled  
10 squares in Fig. 2). Here, we note an alternative means of mismatch discrimination based on the more pronounced response of the mismatched target to an attractive field relative to passive conditions. This different response,  
seen when comparing matched and mismatched kinetics at  
15 open circuit and +300 mV, could have application in real-time detection of mismatch without the need to monitor the full kinetic isotherm.

**Example 5: Electrostatic denaturation, stringency of hybridization and mismatch detection**

20 DNA films containing fully complementary target/probe duplexes or two-base mismatch target/probe duplexes (see Table 1 for sequences) were formed under passive hybridization conditions and then subjected to a repulsive applied potential (-300 mV). The effect of the  
25 applied electrostatic potential on the stability of the duplex films was determined by monitoring loss of ssDNA strands from the surface, Fig. 3, by *in situ* SPR detection in the presence of hybridization buffer (1 M NaCl solution containing 1 μM oligonucleotide target).  
30 The data in Fig. 3 are reported relative to the level of steady state hybridization present at the onset of the

applied field. For the mismatched hybrid, application of a repulsive potential results in rapid denaturation of most (~75%) of the immobilized duplex within a few minutes whereas for the fully complementary hybrid,  
5 relatively little loss of ssDNA is observed even after many hours of exposure to the electrostatic field. Exponential fits to the data (solid lines) indicate that the time constant for denaturation of the mismatch is ~35 times smaller than for the full complement.

10 Similar mismatch discrimination was also observed for targets that contained only 1 bp mismatch out of 25, (see Table 1 for sequences). The discrimination effect is large therefore the mismatch discrimination sensitivity is at least 1 bp mismatch out of 25. This  
15 discrimination sensitivity can be achieved if the assay is performed in the hybridization buffer (that is, with target species in the solution) or in a rinse buffer containing no targets. Mismatch discrimination can be achieved for target solutions or rinse solutions of lower  
20 ionic strength (for example, 0.1 M NaCl), for probe films formed by different methods (see Example 8), and for probe films of different density.

Mismatch discrimination can also be attained by an alternative method of ramping the potential to  
25 increasingly repulsive potentials. The mismatched target is denatured at lower values of the repulsive potential.

The identity of the mismatch may be determined from control experiment by comparing the results of electrostatic denaturation for known targets. More than  
30 one control may be needed to identify the unknown.

Mismatch discrimination is important for many applications such as detection of mutations or single nucleotide polymorphisms in biological samples.

**Example 6: ssDNA vs. dsDNA Immobilization**

5

Comparison of the immobilization of **ss**-DNA-C<sub>6</sub>-SH on gold and **ds**-DNA-C<sub>6</sub>-SH adsorption under the same solution conditions (1M KH<sub>2</sub>PO<sub>4</sub>) is shown in Figure 9. The sequences used are shown in Table 1. For clarity and 10 ease of comparison, the data in Figure 9 are reported in units of molecules/cm<sup>2</sup>.

Over repeated experimental runs, the final coverage for **ds**DNA-C<sub>6</sub>-SH, which is immobilized as a duplex, ~3x10<sup>12</sup> duplexes/cm<sup>2</sup>, is consistently lower than the density 15 achieved for **ss**DNA-C<sub>6</sub>-SH. In addition, the kinetic behavior appears to follow a faster isotherm in contrast to the more complex kinetics for **ss**DNA-C<sub>6</sub>-SH immobilization<sup>16</sup>. The observed difference in the shape of the kinetic isotherms is not yet fully understood but is 20 likely to be due to a combination of effects, including differences in the conformation, flexibility and electrostatic interactions of duplex vs. single stranded DNA under these identical solution conditions.

If we consider only the repulsive electrostatic 25 interaction due to charge along the backbone of the DNA, we might expect duplex immobilization to result in a film with half the **ss**DNA-C<sub>6</sub>-SH probe density, simply because duplex DNA contains twice the anionic charge. The observation that the probe density for duplex 30 immobilization is less than half of that obtained for **ss**DNA-C<sub>6</sub>-SH immobilization, Figure 9, suggests that non-

electrostatic effects such as the conformation or flexibility of the DNA strands may also be factors that control the ultimate probe density.

Benight and coworkers <sup>24</sup> report 40% larger probe coverage for the immobilization of linear (single strand) DNA probes compared to hairpin DNA probes. While different attachment chemistry is used, their results are consistent with our observations of achieving greater ssDNA probe density compared to duplex DNA under the same solution conditions. We assume here that hairpin oligonucleotides can be viewed as analogous to duplex DNA with regard to properties such as charge density and flexibility.

Over repeated experimental runs there is some variability in the resulting probe coverage. Interestingly, this variability is greatest for duplex immobilization. The average coverage for duplex immobilization is  $2.8 \times 10^{12} \pm 0.6 \times 10^{12}$  molecules/cm<sup>2</sup>. In contrast, for the case of ssDNA-C<sub>6</sub>-SH immobilization, the average coverage shows much less variability between runs ( $11 \times 10^{12} \pm 0.2 \times 10^{12}$  molecules/cm<sup>2</sup>). The average coverage for both cases is calculated after 10 hours of exposure and the standard deviation is from 6 runs. For both cases, the variability in final probe coverage is not accompanied by a variation in the shape of the isotherm, which remains highly consistent between runs. The variability in the magnitude of the measured coverage is most likely caused by sample-to-sample variations in the gold surface roughness. Although there are no systematic studies of surface roughness on probe density, some data<sup>25</sup> suggest that higher probe densities are reached on rougher surfaces. This is mainly due to the greater

available area for probe attachment on rough surfaces. At this time it is not understood why duplex DNA immobilization shows greater variability in probe density from run to run.

5

**Example 7: Ionic Strength Dependence of Immobilization**

The kinetics of immobilization depend strongly on solution ionic strength for both **dsDNA-C<sub>6</sub>-SH**, Figure 6A, 10 and **ssDNA-C<sub>6</sub>-SH**, Figure 6B. In low ionic strength solutions, we observe less probe adsorption because of the larger electrostatic repulsion between probe strands. In high ionic strength solutions, the electrostatic repulsions between probe molecules are effectively 15 screened, and higher probe coverages can be reached. These results are consistent with observations made by Tarlov and coworkers,<sup>5</sup> who report that maximum probe coverage is achieved when the KH<sub>2</sub>PO<sub>4</sub> concentration is greater than 0.4 M. We have found that immobilization in 20 either 1 M KH<sub>2</sub>PO<sub>4</sub> (pH 4) or 1 M NaCl (pH 7.2 w/TE buffer) show similar kinetics of film formation and similar final probe densities (not shown).

A more subtle effect, that has not been reported previously, arises in the shapes of the adsorption 25 isotherms. When the data in Figure 6 are scaled (not shown) it is clear that the rate of probe adsorption in the first few hours is consistently slower at lower ionic strength compared with adsorption in high ionic strength solution. Probe immobilization involves an interplay of 30 forces including the short range chemical interactions of the covalent gold/thiol attachment and the long range electrostatic repulsion between DNA strands. In these

experiments the electrostatics dominate: when the Debye length is large, the rate of probe attachment is low.

**Example 8:** Electrostatic Field Control of Probe  
5 Immobilization

We have discovered that an applied electrostatic field can control probe immobilization and is a strategy for controlling DNA probe density. Interestingly, for 10 n-alkanethiols on gold, Lennox and coworkers <sup>26</sup> have shown that potential-assisted deposition leads to a faster and ultimately more complete self-assembled monolayer formation process. Here, we show that potential-assisted deposition can dramatically alter the process of 15 attachment of thiol DNA to gold, Figure 7. In related work from our laboratory, we have found that electrostatic fields can alter the rate of hybridization and denaturation <sup>15</sup>.

Figure 7 shows the effect of applying a potential of 20 +0.3V vs. Ag/AgCl to the gold surface during the immobilization of ssDNA-C<sub>6</sub>-SH. Electrostatically controlled immobilization (closed triangles) has a larger initial rate of adsorption than ssDNA-C<sub>6</sub>-SH immobilization in the absence of an applied potential (open circles) 25 under the same solution conditions. In the presence of the positive applied potential, the maximum attainable surface coverage remains similar to coverage attained at open circuit but the rate is enhanced. Probe films formed by potential-assisted deposition are covalently 30 attached; there is no significant probe loss when the potential is removed or when the film is rinsed. Target-

capture rates for probe films formed with and without potential assistance are compared in Section III.

Figure 11 shows how electrostatic fields can be used for controlling the extent of immobilization or attachment of biomolecules, such as thiol-derivatized oligonucleotides. This method of patterning (selectively assisting or preventing immobilization in a specific region of the surface) can be used not only on bare gold SPR sensors but also on chemically modified surfaces. It is important to note that probe coverage only increases during the attractive pulse and little if any immobilization is observed while the repulsive potential is applied despite the fact that the solutions used for these electrostatically assisted immobilization experiments contain 1  $\mu$ M concentration of the desired probe ssDNA-C<sub>6</sub>-SH. That is, the spontaneous self-assembly of the ssDNA-C<sub>6</sub>-SH probe is arrested by the application of a repulsive potential. This approach is useful for attaching biomolecule probes to bare surfaces or chemically modified surfaces, that is, surfaces coated with monolayer or multilayer films formed by a variety of known methods, such self-assembled monolayer techniques.

**Example 9: Probe density effects on probe/target hybridization**

Probe density strongly affects target hybridization efficiency, that is, for high probe density films, we find that the efficiency of hybridization is low, Figure 8. For these data, the probe density was controlled by varying the exposure time of the gold surface to ssDNA-C<sub>6</sub>-SH during the probe film fabrication process. For each hybridization isotherm shown in Figure 8, target/probe

hybridization was performed under the same conditions of solution concentration and ionic strength. The efficiency of hybridization after 30 minutes varies from about 15 % to 95% depending on the probe density, with 5 the highest density films exhibiting the lowest efficiencies. Longer exposure to target solutions for up to 14 hours increases the efficiency of hybridization somewhat: the range becomes 30% to almost 100%.

Our results are in general agreement with the 10 amount of probe/target hybridization reported by other groups. For example, Demers et. Al <sup>27</sup> used a fluorescence based measurement to detect probe coverage and target hybridization on planar gold. For overnight immobilization, which is likely to lead to high-density 15 probe coverage, the reported target hybridization efficiency for the resulting film was 33% even after 40 hours, comparable to our observations. Steel et. al. used an electrochemical detection approach to observe a trend similar to our observations, that is, high density 20 probe films have reduced target hybridization efficiency <sup>21</sup>.

Previous heating of the probe surface appears to have a significant effect on the hybridization efficiency. For example, a 22% increase in hybridization 25 efficiency was observed (solid circles in Figure 8) when compared with the efficiency on a never heated surface. A similar increase was observed for a higher density film, as reported previously for a different 25-mer sequence <sup>7</sup>. This was not due to probe loss since there is 30 no measurable decrease in probe coverage. At very high probe densities, prior probe heating does not improve the efficiency of hybridization.

If we focus on the shape of the kinetic isotherms, we see that the kinetics of hybridization also have a distinct dependence on probe density. This effect, which is due likely to intermolecular interactions, has 5 not been observed previously. Trends in the data are most clearly visualized when the kinetic isotherms are normalized, as in Figure 9. The data appear to fall into different regimes depending on the probe densities. For probe densities below  $\sim 3 \times 10^{12}$  molecules/cm<sup>2</sup> the initial 10 hybridization rate was faster reaching a maximum within  $\sim 15$  minutes. The distinct shape of the hybridization isotherms at high densities above  $\sim 5 \times 10^{12}$  molecules/cm<sup>2</sup> (slower target capture rate) is due most likely to repulsive electrostatic and steric interactions that 15 increase with increasing probe density.

The fact that probe density can alter target capture rates is not unexpected but is not often considered, especially when differential measurements are made where the magnitudes of probe immobilization or hybridization 20 are not recorded but only the ratio of matched to mismatched duplexes. It is interesting to note that the kinetics of hybridization for matched and mismatched DNA are distinct,<sup>8</sup> however, it is not yet known whether probe density influences matched and mismatched duplex 25 formation to the same degree. The influence of probe density on the formation perfectly matched vs. partially mismatched hybrids is the subject of ongoing work in our laboratory.

In some cases, differences in probe density are 30 measured, for example in the work of Benight and coworkers<sup>24</sup> who propose that DNA hairpins could offer substantial advantages as nucleic acid capture moieties in

solid support based hybridization systems. They observe capture rates that depend on whether a linear or hairpin DNA probe is used and attribute the difference in kinetics to the increased stability of the hairpin 5 probe/target duplex structure. However, the coupling density for linear probes is nearly twice that for hairpin probes. Based on our results, we would predict lower rates of target capture for higher density probe 10 films. Thus, the higher density of the linear probe films could account, at least in part, for the different observed rates.

**Example 10:** Comparing probe films formed by different immobilization strategies

In this example, we compare the effectiveness of DNA 15 probe films fabricated using different immobilization conditions by measuring 1) the rate of hybridization with targets and 2) the overall efficiency of probe/target hybridization. In Figure 10, we compare the kinetics of hybridization on two sets of probe films (low density and 20 high density probe). Low probe densities were obtained by immobilizing **ssDNA-C<sub>6</sub>-SH** for a short time period (<1.5 hours) or via **dsDNA-C<sub>6</sub>-SH** immobilization followed by thermal dehybridization. High probe densities were obtained by immobilizing **ssDNA-C<sub>6</sub>-SH** for a longer time 25 (>10 hours) or via potential-assisted deposition of **ssDNA-C<sub>6</sub>-SH**. The hybridization conditions are identical for both sets of probe films. We observe no difference in the rate, magnitude or efficiency of hybridization for the films formed by a variety of methods provided that 30 probe films of the same probe density are compared.

Those with expertise in this technology will recognize variations of the above that are consistent with the invention disclosed.

## 5 REFERENCES

1. Lockhart, D. J. & Winzeler, E. A. Genomics, gene expression and DNA arrays. *Nature* **405**, 827-836 (2000).
- 10 2. Fodor, S. P. A. DNA sequencing - Massively parallel genomics. *Science* **277**, 393-& (1997).
3. Cantor, C. R. & Smith, C. L. *Genomics: the science and technology behind the human genome* (John Wiley & Sons, Inc., New York, 1999).
- 15 4. Sosnowski, R. G., Tu, E., Butler, W. F., O'Connell, J. P. & Heller, M. J. Rapid determination of single base mismatch mutations in DNA hybrids by direct electric field control. *Proceedings of the National Academy of Sciences of the United States of America* **94**, 1119-1123 (1997).
- 20 5. Herne, T. M. & Tarlov, M. J. Characterization of DNA probes immobilized on gold surfaces. *Journal of the American Chemical Society* **119**, 8916-8920 (1997).
- 25 6. Levicky, R., Herne, T. M., Tarlov, M. J. & Satija, S. K. Using self-assembly to control the structure of DNA monolayers on gold: A neutron reflectivity study. *Journal of the American Chemical Society* **120**, 9787-9792 (1998).
- 30 7. Peterlinz, K. A. & Georgiadis, R. M. Observation of hybridization and dehybridization of thiol- tethered

DNA using two-color surface plasmon resonance spectroscopy. *Journal of the American Chemical Society* **119**, 3401-3402 (1997).

8. Peterson, A. W., Heaton, R. J. & Georgiadis, R.  
5 Kinetic control of hybridization in surface immobilized DNA monolayer films. *Journal of the American Chemical Society* **122**, 7837-7838 (2000).

9. Steel, A. B., Herne, T. M. & Tarlov, M. J.  
10 Electrostatic interactions of redox cations with surface-immobilized and solution DNA. *Bioconjugate Chemistry* **10**, 419-423 (1999).

10. Schlereth, D. D. Characterization of protein monolayers by surface plasmon resonance combined with cyclic voltammetry 'in situ'. *Journal of Electroanalytical Chemistry* **464**, 198-207 (1999).

11. Boussaad, S., Pean, J. & Tao, N. J. High-Resolution Multiwavelength Surface Plasmon Resonance Spectroscopy for Probing Conformational and Electronic Changes in Redox Proteins. *Anal. Chem.* **72**, 222 -226 (2000).

20 12. Badia, A. et al. Probing the electrochemical deposition and/or desorption of self-assembled and electropolymerizable organic thin films by surface plasmon spectroscopy and atomic force microscopy.  
25 *Sensors and Actuators B-Chemical* **54**, 145-165 (1999).

13. Georgiadis, R., Peterlinz, K. A., Rahn, J. R.,  
30 Peterson, A. W. & Grassi, J. H. Surface plasmon resonance spectroscopy as a probe of in-plane polymerization in monolayer organic conducting films. *Langmuir* **16**, 6759-6762 (2000).

14. Hodneland, C. D. & Mrksich, M. Biomolecular surfaces that release ligands under electrochemical control.

*Journal of the American Chemical Society* **122**, 4235-4236 (2000).

15. Heaton, R. J., Peterson, A. W. & Georgiadis, R. M. Electrostatic surface plasmon resonance: Direct electric field-induced hybridization and denaturation in monolayer nucleic acid films and label-free discrimination of base mismatches. *Proceedings of the National Academy of Sciences of the United States of America* **98**, 3701-3704 (2001).

10 16. Georgiadis, R., Peterlinz, K. P. & Peterson, A. W. Quantitative measurements and modeling of kinetics in nucleic acid monolayer films using SPR spectroscopy. *Journal of the American Chemical Society* **122**, 3166-3173 (2000).

15 17. Forman, J. E., Walton, I. D., Stern, D., Rava, R. P. & Trulson, M. O. (eds.) *Thermodynamics of duplex formation and mismatch discrimination on photolithographically synthesized oligonucleotide arrays* (1998).

20 18. Peterlinz, K. A. & Georgiadis, R. In situ kinetics of self-assembly by surface plasmon resonance spectroscopy. *Langmuir* **12**, 4731-4740 (1996).

19. Peterlinz, K. A. & Georgiadis, R. Two-color approach for determination of thickness and dielectric constant of thin films using surface plasmon resonance spectroscopy. *Optics Communications* **130**, 260-266 (1996).

25 20. Peterson, A. W., Heaton, R. J. & Georgiadis, R. The effect of surface probe density on DNA hybridization. *Nucleic Acids Research* **29**, 5163-5168 (2001).

21. Steel, A. B., Herne, T. M. & Tarlov, M. J. Electrochemical quantitation of DNA immobilized on gold. *Analytical Chemistry* **70**, 4670-4677 (1998).
22. Mbainyo, J. K. N. et al. DNA-directed assembly of gold nanowires on complementary surfaces. *Advanced Materials* **13**, 249-+ (2001).
23. McIntyre, J. D. E. & Kolb, D. M. Specular reflection spectroscopy of electrode surface films. *Symp. Faraday Soc.* No. **4**, 99-113 (1970).
- 10 24. Riccelli, P. V. et al. Hybridization of single-stranded DNA targets to immobilized complementary DNA probes: comparison of hairpin versus linear capture probes. *Nucleic Acids Research* **29**, 996-1004 (2001).
- 15 25. Huang, E., Satjapipat, M., Han, S. B. & Zhou, F. M. Surface structure and coverage of an oligonucleotide probe tethered onto a gold substrate and its hybridization efficiency for a polynucleotide target. *Langmuir* **17**, 1215-1224 (2001).
- 20 26. Ma, F. Y. & Lennox, R. B. Potential-assisted deposition of alkanethiols on Au: Controlled preparation of single- and mixed-component SAMs. *Langmuir* **16**, 6188-6190 (2000).
27. Demers, L. M. et al. A fluorescence-based method for determining the surface coverage and hybridization efficiency of thiol-capped oligonucleotides bound to gold thin films and nanoparticles. *Analytical Chemistry* **72**, 5535-5541 (2000).

## CLAIMS

What is claimed is:

5        1. A method for assaying a biological target using surface plasmon resonance, said method comprising:

      a. attaching a probe for said biological target onto a surface,

10      b. bringing said surface into contact with a solution containing a sample of said biological target,

      c. generating a locally resolved curve from a surface plasmon resonance detector, said curve obtained during application of voltage to determine the pattern for probe target binding vs. time or voltage, and

15      d. comparing said pattern of probe target binding for said biological target to that of a control.

20        2. The method of claim 1 wherein said voltage is such that there is no Faradaic current.

25        3. The method of claim 2 wherein said biological target is selected from the group consisting of nucleic acids, proteins and polypeptides and whole cells and parts of cells.

30        4. The method of claim 3 wherein said nucleic acid is an oligonucleotide.

35        5. The method of claim 2 wherein said assay is a qualitative assay, said method comprising using a control having a known identity.

6. The method of claim 2 wherein said assay is a quantitative assay, said method comprising using a control having known identity and concentration.

5 7. The method of claim 2 wherein said surface comprises pure or chemically modified gold, silver, copper, or semiconductor.

8. The method of claim 2 wherein applied voltage  
10 is used to attach said probes to said surface.

9. The method of claim 8 wherein said voltage quantitatively controls the amount of probe attached to said surface.

15

10. The method of claim 8 wherein SPR is used to confirm the attachment of said probe.

11. The method of claim 4 wherein the mismatch  
20 discrimination is at least 1 base pair in 25.

12. The method of claim 11 wherein said mismatch discrimination can be used to determine the identity of said biological target.

25

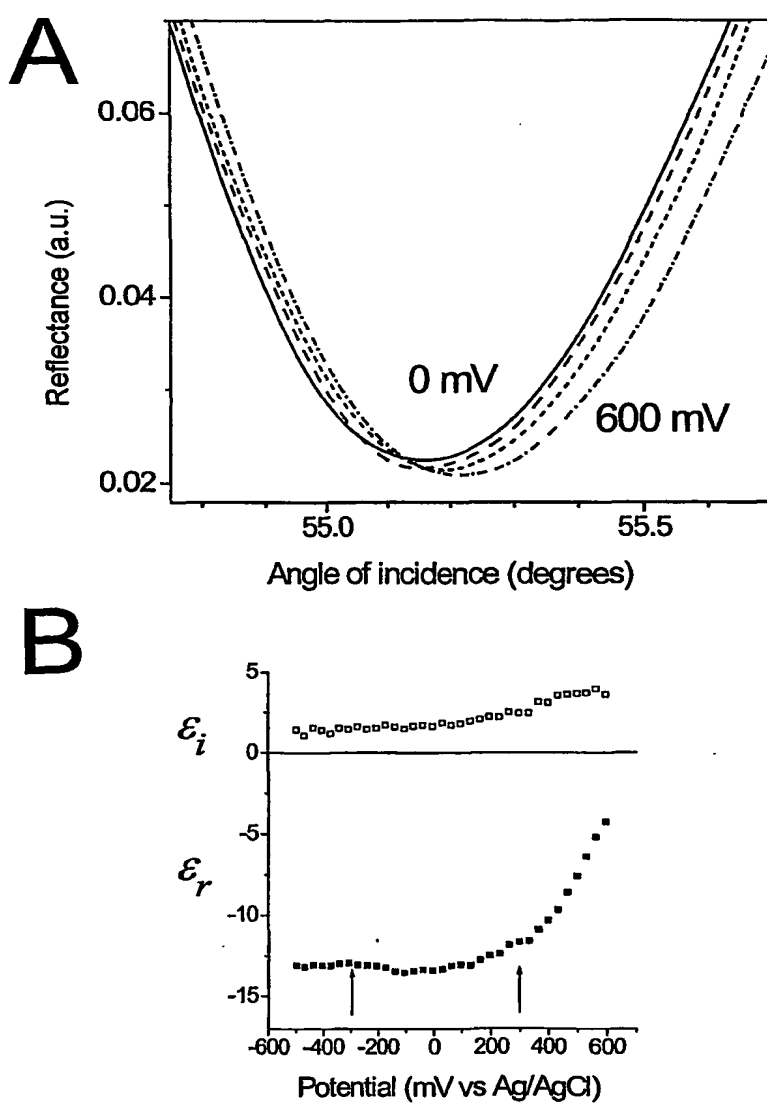
13. The method of claim 1 wherein said locally resolved curve is determined before and after the application of said voltage.

30

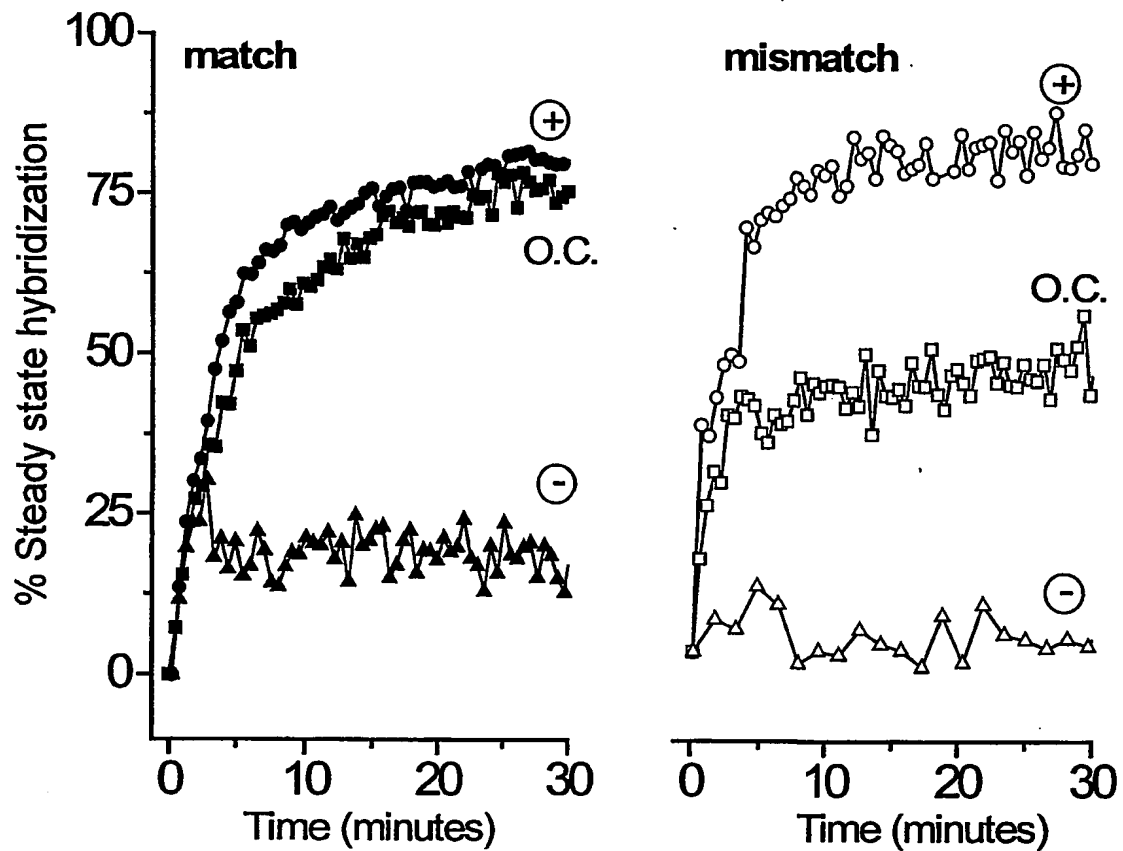
14. The method of claim 1 wherein said locally resolved curve is used in its entirety.

15. The method of claim 1 wherein a portion of said locally resolved curve is used.

1/11

**Figure 1**

2/11

**Figure 2**

3/11

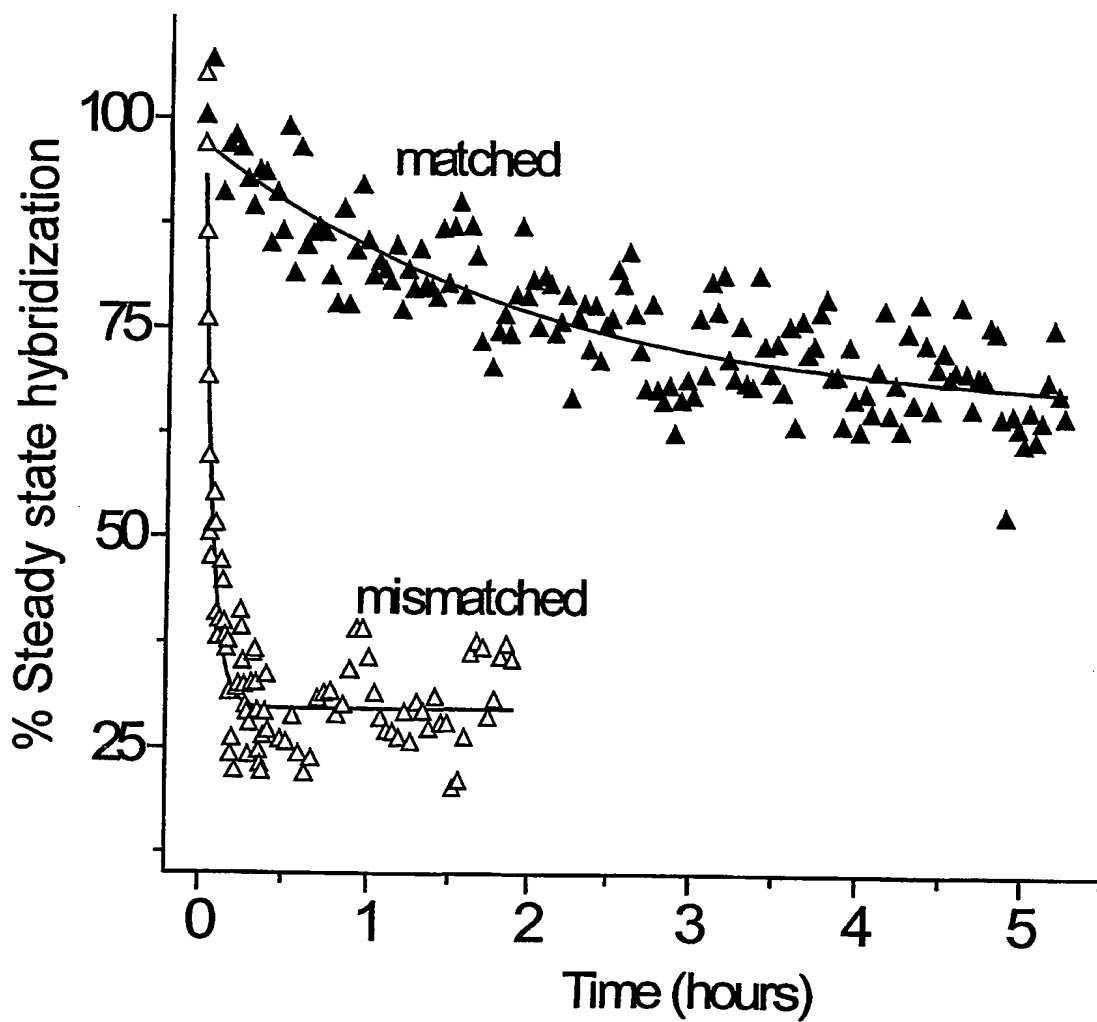
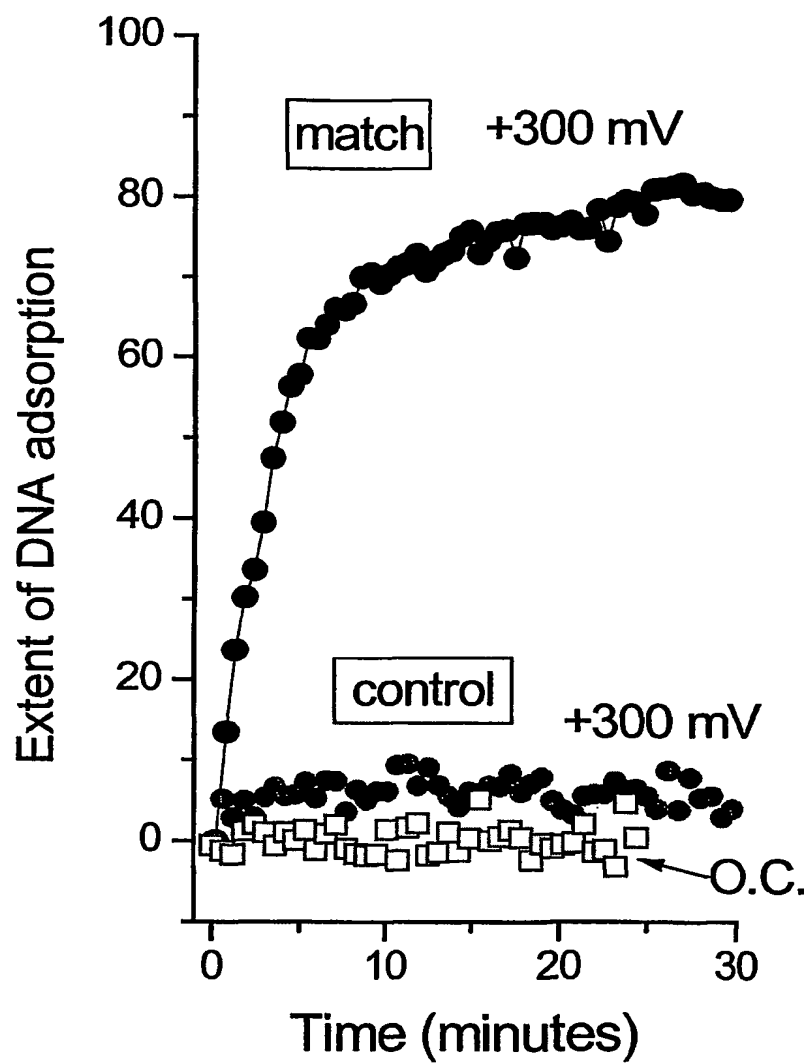
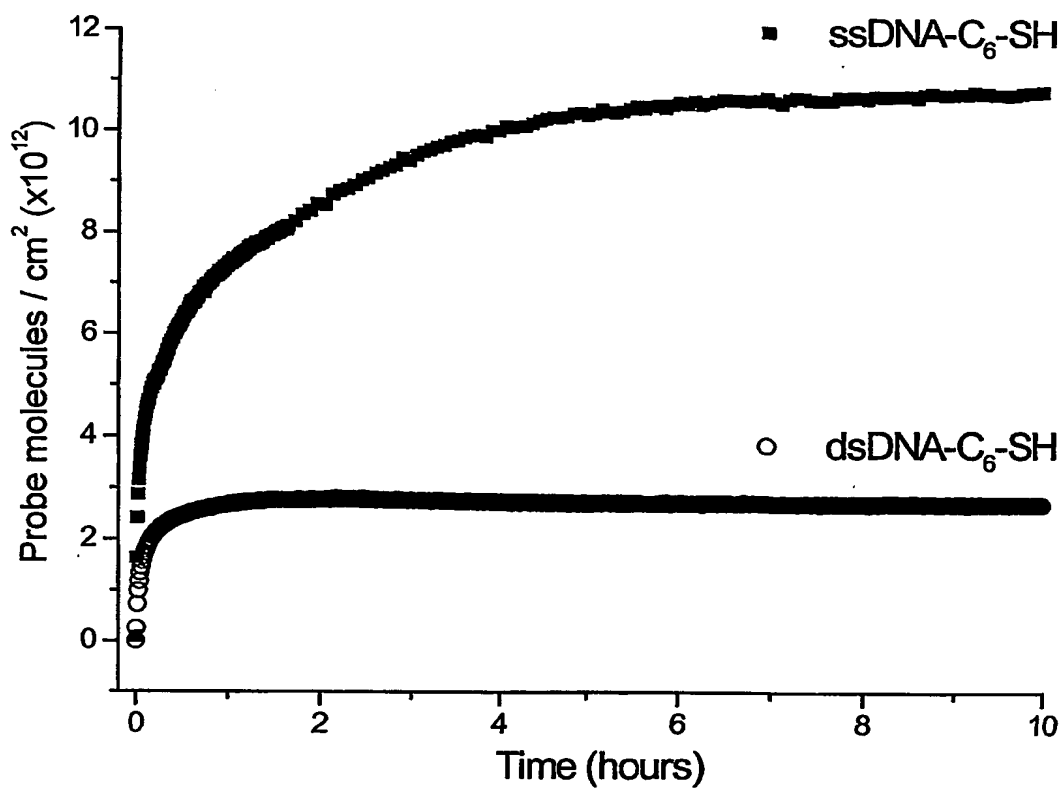


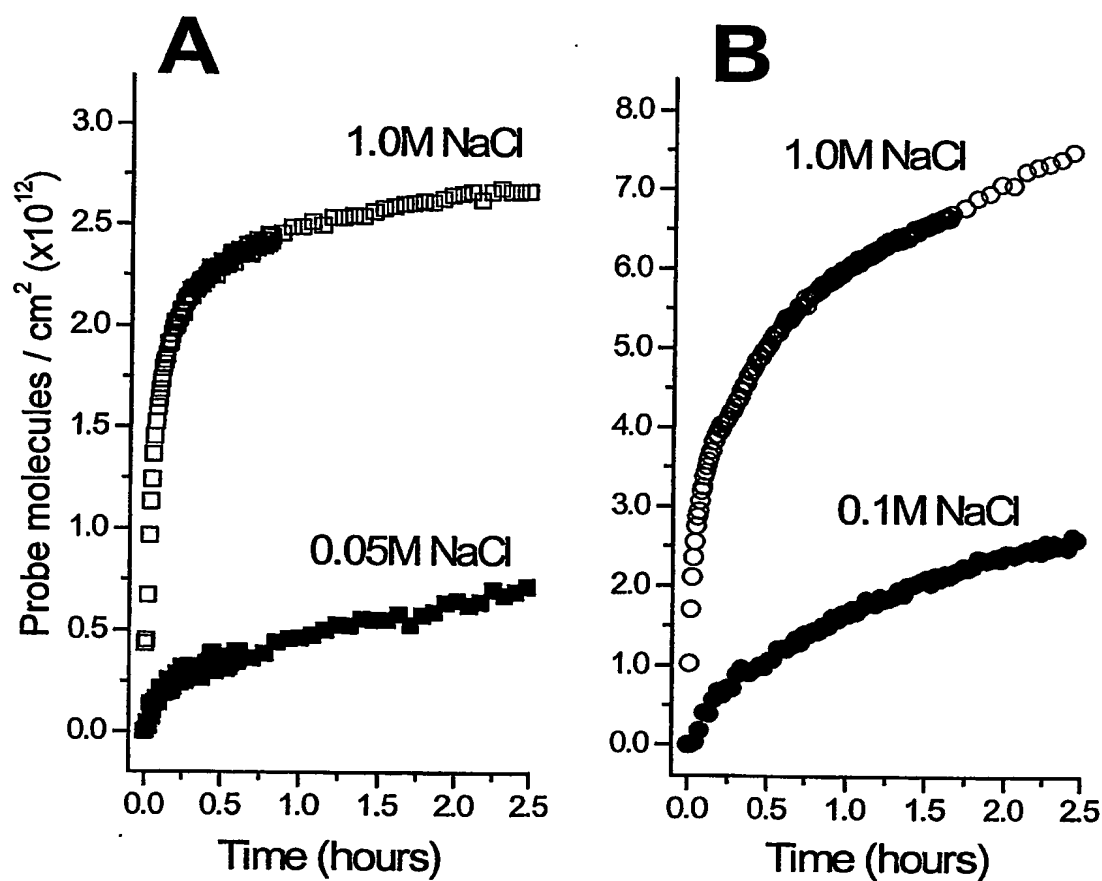
Figure 3

4/11

**Figure 4**

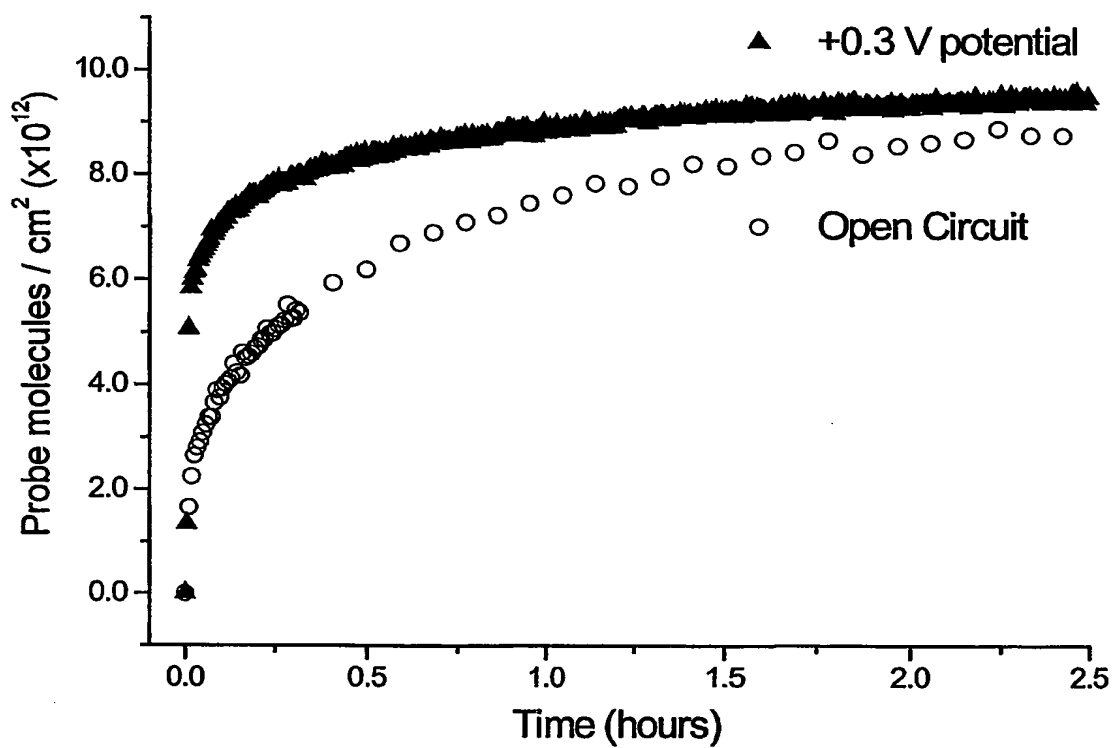
5/11

**Figure 5**



**Figure 6**

7/11

**Figure 7**

8/11

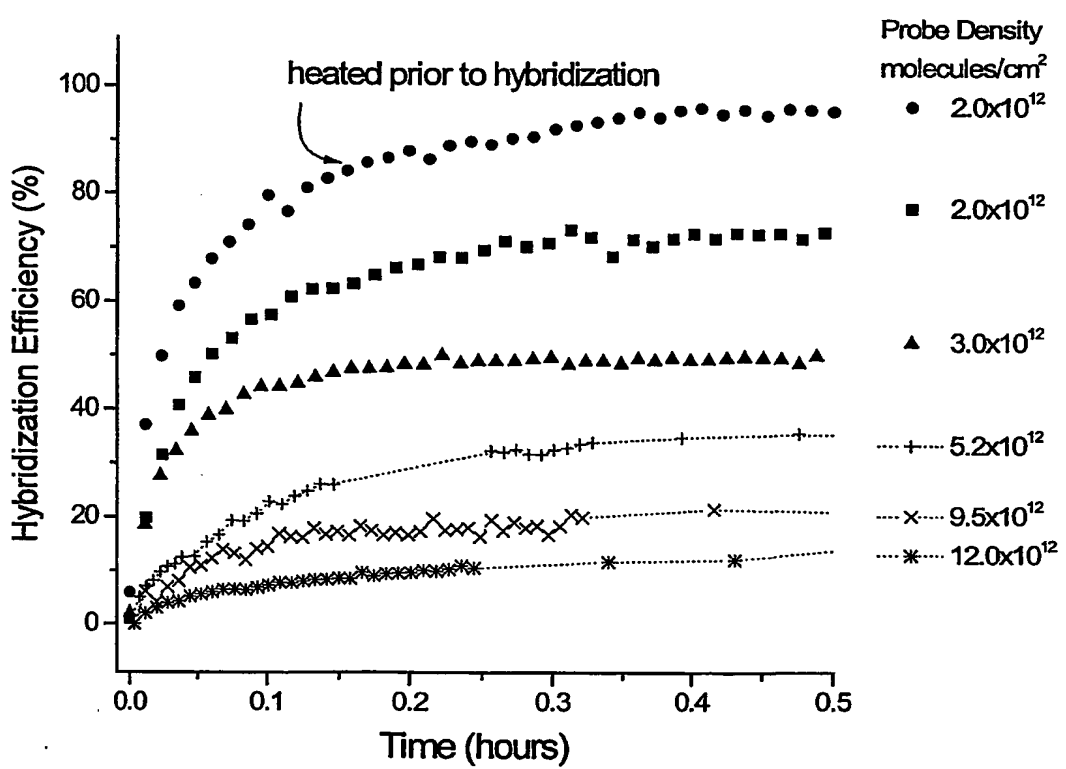


Figure 8

9/11

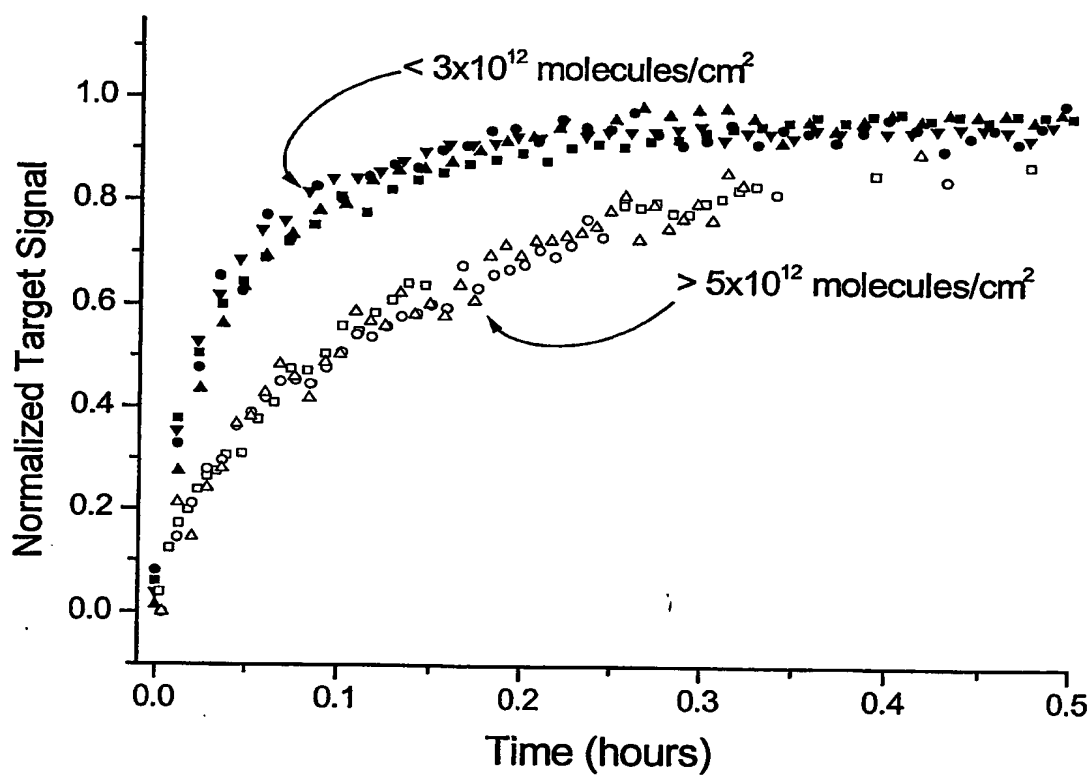
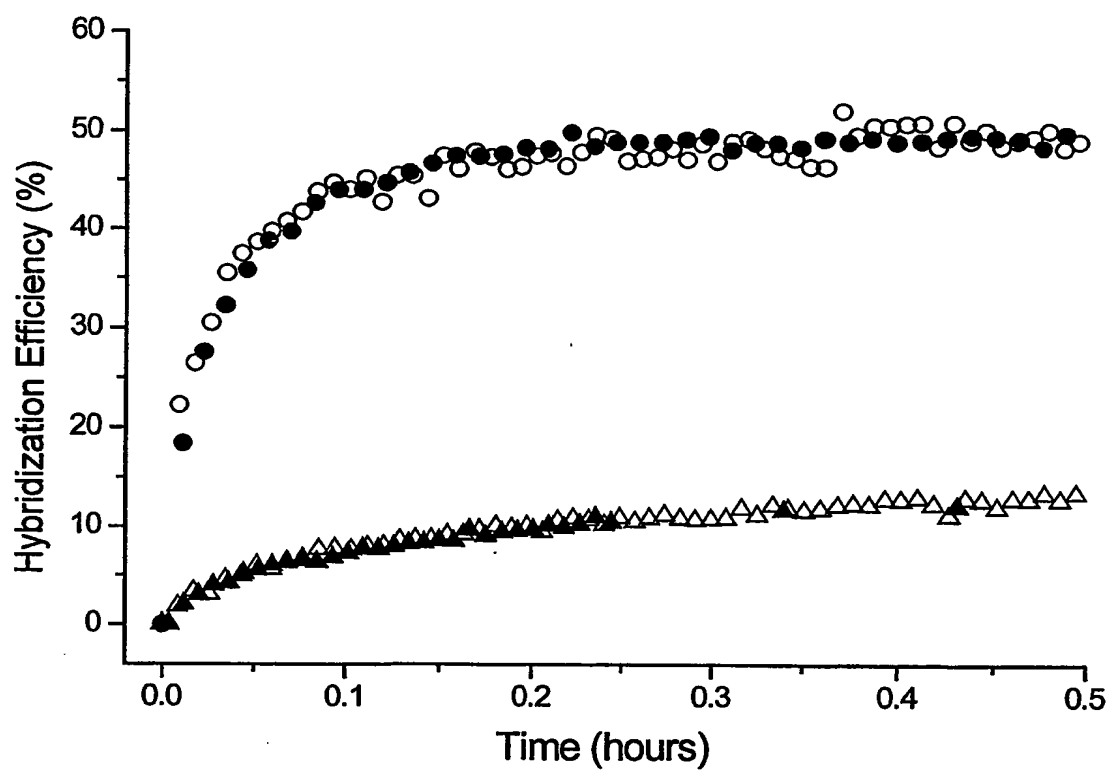
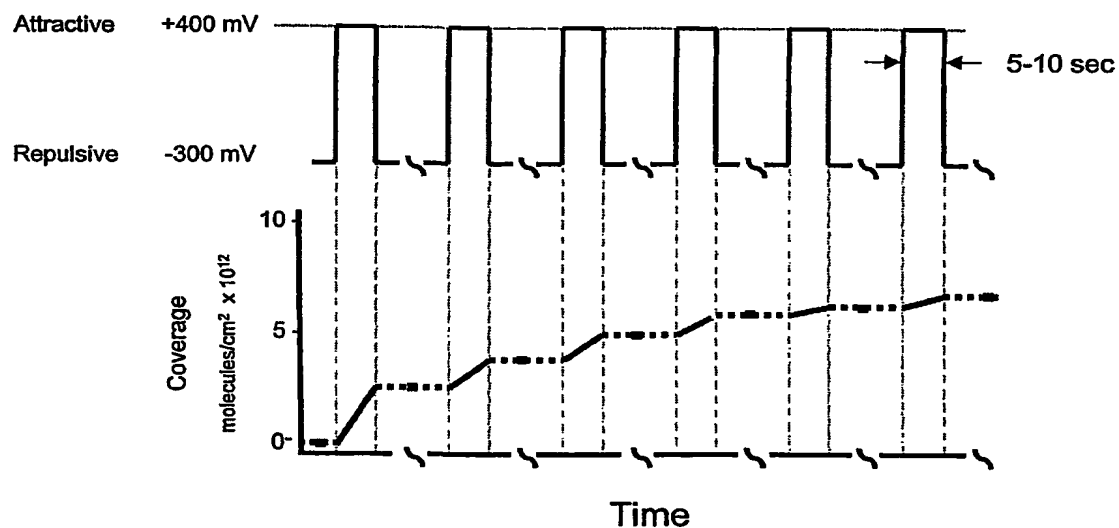


Figure 9

10/11

**Figure 10**

11/11

**Figure 11**